JOURNAL OF APPLIED POLYMER SCIENCE VOL. 19, PP. 1029–1035 (1975)

# The Structural Color in the Polymer Blend of Poly(methyl Methacrylate) and Polystyrene

YUKIKAZU UEMURA and MASAYA AOYAGI, *Central Research Laboratory, Sumitomo Chemical Company, Takatsuki City, Osaka, Japan*

## Synopsis

Morphologic and optical studies were performed on the coloring of poly(methyl methacrylate) (PMMA) and polystyrene (PS) opal sheet. It was concluded that the origin of color is the polymer structure itself. There exist three structures in the colored polymer blend: small PS spheres are dispersed in the PMMA matrix, and each PS sphere contains smaller PMMA spheres within it. The dimension of the smaller PMMA spheres is of the same order as the wavelength of visible or near-infrared light. The coloring measured by a spectrometer is well interpreted by the equation of structural color derived by Clewell qualitatively.

## INTRODUCTION

A mixture of polymers of different refractive indexes becomes opaque, owing to light scattering. This is the opal effect. The ideal opal sheet scatters light uniformly and does not change the spectral distribution of the incident light. In some cases, however, an opal sheet appears slightly brown when it is illuminated by white light, even though the component polymers are transparent.

The first observations of the light scattering by a particle were made by Tyndall,[1] and general light scattering theory by a sphere was developed by Mie[2] and Debye[3] and summarized by Oster[4] and Van der Hulst.[5] Light scattering in crystalline polymer has been extensively studied by Stein,[6] Kawai,[7] and other workers,[8] but a color phenomenon mentioned above seems not to have been reported so far in polymers. On the other hand, Clewell et al.[9–11] observed coloring due to microstructures in inorganic pigments dispersed in water. Accordingly, they called the effect "structural coloring." The attempt was made to apply this treatment in order to elucidate the mechanism of coloring in the polymer mixtures. The result was found to be quite successful.

## EXPERIMENTAL

Sample A, in which 3 wt-% of polystyrene (PS) homopolymer was blended into PMMA, has relatively strong coloring, while sample B for which the same per cent of styrene and methyl methacrylate copolymer was blended, has a slight color. In order to observe the microstructures in the blends, an electron microscope (EM) and a scanning electron microscope (SEM) were used. Electron micrographs were taken by the two-step replica method developed by Heidereich

et al.[12] As it was found that PS part is swollen by isopropanol more easily than PMMA, the sample was immersed in isopropanol at 65°C for 60 min. The first replica of the swollen sample was prepared by poly(vinyl alcohol) (PVA). Then the carbon coating was made on its surface to a thickness of 300 Å, and subsequently the PVA substrate was dissolved into water to give the second replica. For the EM observation, chromium was evaporated on the second replica surface from the low angle in order to get good contrast shadowing.

The electron microscope was a Model HU-11B, Hitachi Co. The scanning electron microscope was a Model JSM-2, Japan Electron Optics Co.

The light scattering within the sample occurred in near-infrared (NIR) and ultraviolet (UV) regions as well as in the visible (VIS) region. A Perkin-Elmer 450 UV-VIS spectrophotometer and a Hitachi-Perkin 125 IR spectrophotometer were used for the optical measurements. For the measurement, another PMMA sheet which was polished to the same thickness as the opal sheet was inserted in the reference side of the spectrophotometer to cancel out the molecular absorption by PMMA.

## RESULTS

The structures of samples A and B observed by the EM and SEM are shown in Figure 1. The PS parts swollen by isopropanol are seen as spheres which are dispersed in the PMMA "sea."

In the case of sample A (Figs. 1a and 1c), the dispersed PS spheres of about 3 $\mu$ contain PMMA spheres of smaller sizes. Comparing the EM with SEM pictures, it is clear that the two-step replica method transfers the structures of the sample correctly.

Polystyrene latex of uniform radius of 0.234 $\mu$ (Dow Chemical Co.) was sprayed on the second replica surface to examine whether the inner structure is concave or convex to the surface (Fig. 2). The direction of the shadow of the inner PMMA sphere is the same as that of the PS latexes, and it is concluded that the PS part containing PMMA secondary structures is higher than the PMMA sea due to the swelling.

The distribution of the inner PMMA sphere radii is shown in Figure 3. The maximum locates around 0.1–0.3 $\mu$ and the average radius $\bar{d}$ is 0.325 $\mu$. The

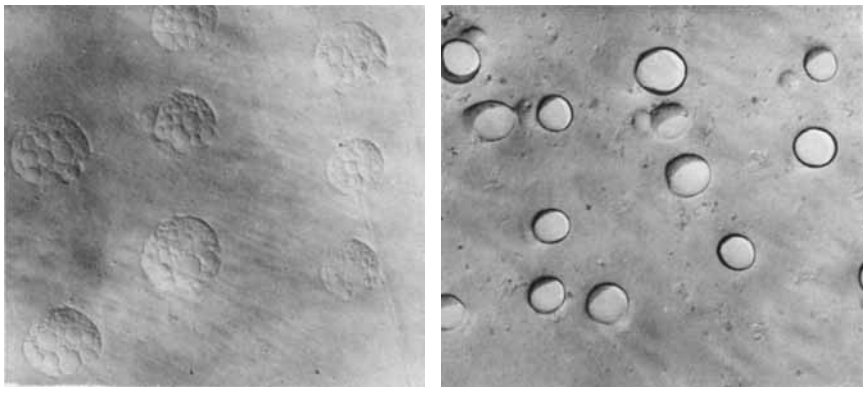

(a) (b)

Fig. 1 (*continued*)

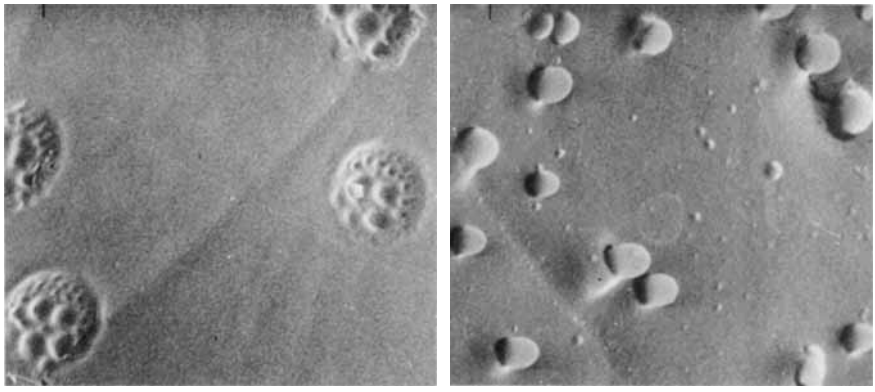

(c) (d)

Fig. 1. Electron and scanning electron micrographs: (a) EM of sample A (×2500); (b) EM of sample B (×4500); (c) SEM of sample A (×5000); (d) SEM of sample B (×5000).

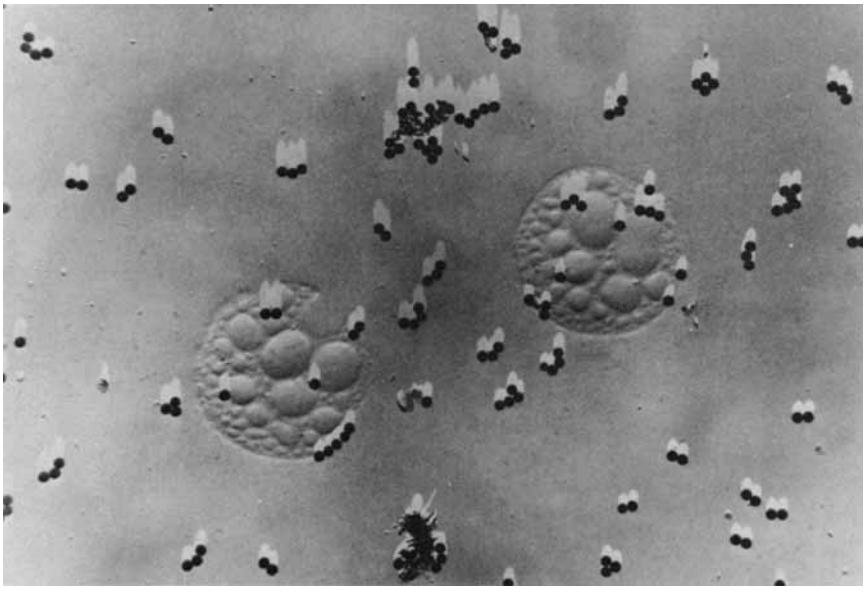

Fig. 2. Electron micrograph of sample A. PS latexes of uniform radius of 0.234 $\mu$ are sprayed on the second replica surface (×4060).

distribution curve tails to the larger radius up to 1.1 $\mu$, just like the one reported by Reinhold.[13]

For sample B, however, no secondary structures can be seen in the PS sphere (Figs. 1b and 1d), which must be atrributed to the better solubility of styrene–methyl methacrylate copolymer to PMMA, and the coloring is not as much as that of sample A.

The absorption curves of the samples in the region from UV to NIR are shown in Figure 4a (sample A, thickness $l$ = 0.237 mm) and Figure 5a (sample B, $l$ = 2.065 mm). The apparent "absorption" of the opal sheet, in the true sense the light loss by the scattering, extends to the region from UV to IR. The scattering in the short wavelength is stronger than that in the long wavelength. This is

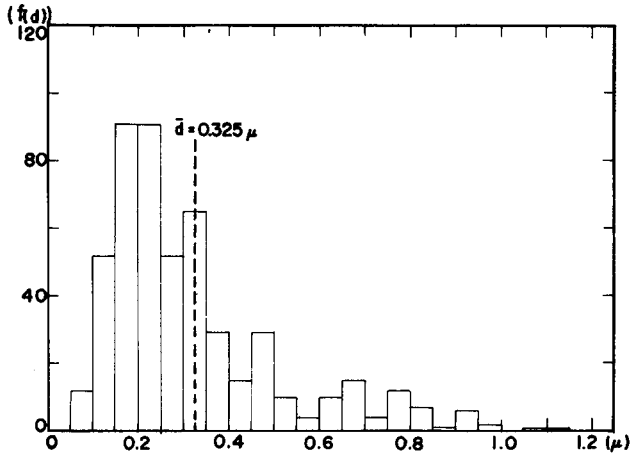


Fig. 3. Distribution of inner PMMA sphere radii of sample A.

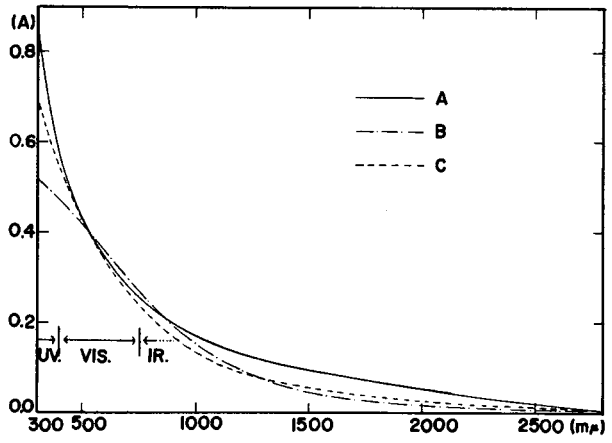


Fig. 4. Absorbance curves of sample A: (A) experimental; (B) calculated using eq (3) assuming $d = 0.325\ \mu$; (C) calculation of eq. (5) weighted by the distribution $f(d_i)$ of Fig. 3.

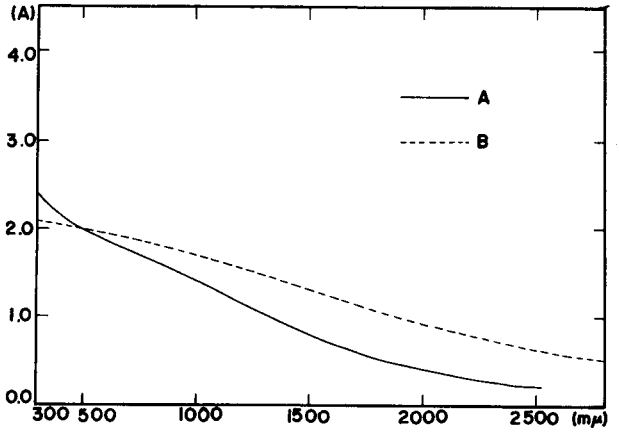


Fig. 5. Absorbance of sample B: (A) experimental; (B) calculated.

responsible for the slight brown color of the polymer blends discussed. The difference of the absorbance at 400 mμ and 750 mμ (visible region) per unit thickness of sample A is larger than that of sample B, which corresponds to the difference of their degree of coloring.

## DISCUSSION

Both PMMA and PS are transparent plastics in the visible region. When several per cent of PS are dispersed in PMMA, however, the blend system becomes opaque. Different from the molecular absorption when observed by a spectrometer, the apparent "absorption" extends in the whole wavelength region. But actually, the while light transmitted from the opal sheet colors slightly brown. As is shown in Figure 4, the scattering is strong in the short wavelength, so that the longer wavelength component (red or yellow color) increases in the transmitted light. Light scattering theory was applied to explain such a coloring phenomenon.

The intensity of light scattering by a much smaller particle than the wavelength is expressed by the equation of Rayleigh,[14] the special case of the more general Mie[2] result. The scattering intensity $S^0$ of the polarized light in the direction $(\varphi,\chi)$ to the incident beam is expressed under the condition of $(n-1)\cdot d/2 \ll 1$,

$$S^0(\varphi,\chi) = \frac{\pi\alpha^4\cdot d^3\cdot\eta}{8r^2m^3}(1-\sin^2\chi\cdot\cos^2\varphi)\cdot J^2_{3/2}(m) \tag{1}$$

where $d$ = particle radius; $\eta = 9\left(\frac{n^2-1}{n^2+2}\right)^2$; $n = n_1/n_0$; $n_0$ = refractive index of surrounding material; $n_1$ = refractive index of scattering material; $\alpha = \pi d\cdot n_0/\lambda$; $m = 2\alpha\cos\chi/2$; $r$ = distance from the scattering material; and $\lambda$ = wavelength of light.

For the unpolarized light (natural light), eq. (1) can be integrated in the whole direction, and the scattering intensity $S'$ is given by

$$S' = \eta\cdot d^3/(\lambda\cdot n_0)^4. \tag{2}$$

The scattering is inversely proportional to $\lambda^4$, and the shorter wavelength is scattered more strongly.

When the scattering material approaches the same dimension as the wavelength, the light scattering becomes affected by the diffraction. Then the light with the same wavelength as the dimension of the scattering particle is scattered selectively. The relations are given by the eq. (3), assuming the damped oscillator model and diffraction scattering[9]:

$$S^* = \frac{1/d}{((0.61\cdot\lambda/n_0\cdot d)^2-1)^2+\kappa} \tag{3}$$

where $\kappa$ = damping constant. Maximum scattering occurs at $\lambda$, which corresponds to $\theta$ (half-apex angle of diffracted light cone) = $\pi/2$, where $\sin\theta = 0.61\cdot\lambda/n_0\cdot d$.

Clewell combined eqs. (2) and (3) semiempirically and tried to explain the coloring phenomena in the case of white inorganic pigments dispersed in water with success. According to the theory, the scattering intensity $S(\lambda,d)$ is given by

$$S(\lambda,d) = \frac{k[(n^2 - 1)/(n^2 + 2)]^2}{d((0.61 \cdot \lambda/n_0 d)^2 - 1)^2 + \lambda^2/n_0 d \cdot a[(n - 1)^2 + 1/a]} \quad (4)$$

where $a$ = correction factor; and $k$ = proportionality constant.

Equation (4) coincides with the Rayleigh eq. (2) in the limit $d \to 0$ and with eq. (3) for $d$ nearly equal to $\lambda$. The scattering intensity depends on the wavelength. The coloring expressed by eq. (4), which involves the particle size in it is the structural color. Here, the application of this method to polymer system was intended.

Equation (3) can be applied only when the sample is so thin that multiple scattering can be neglected. With particle size distribution $f(d_i)$ as in Figure 3, a little modification of eq. (4) is necessary to get the total scattering intensity. The scattering equation can be summed linearly after weighting by $f(d_i)$:

$$S(\lambda) = \sum_i f(d_i) \cdot S(\lambda,d_i) \quad (5)$$

where $S(\lambda)$ represents the loss of the incident light intensity; and from the macroscopic point of view, it is considered to be proportional to the turbidity of the system. Therefore, the quantity $S(\lambda)$ can be obtained by measuring the transmittance $T$ or absorbance $A$ of the sample through eq. (6):

$$T = \exp - (\beta \cdot S(\lambda) \cdot 1)$$

where $\beta$ = proportionality constant, and

$$A = -\log_{10} T$$

$$= C \sum_i \frac{1}{d_i((0.61\lambda/n_0 d_i)^2 - 1)^2 + \lambda^2/(n_0 d_i a \cdot ((n - 1)^2 + 1/a))} \quad (6)$$

The constant term $C = \beta \cdot k1(n^2 - 1)^2/(n^2 + 2)^2 \log_{10} e$ can be so chosen as to fit the experimental value with the calculated one at one point in the absorption curve. The value of $a$ is chosen as 7.0.[9] Equation (6) is the equation of structural color, when there is the particle size distribution which connects the coloring with the structure of scattering materials through $d_i$.

Strictly speaking, the turbidity which expresses the attenuation of light due to scattering could be measured by observing the reduction of intensity of the incident light beam at an angle of 0°. Actually, the light scattered within an angle of 2° was observed due to the finite-sized aperture of the instrument, and 2° was observed due to the finite-sized aperture of the instrument, and 2° is small enough to assume for the measured apparent turbidity and true turbidity to coincide for the first approximation.

The calculation of eq. (6) by a computer was compared to the experimental value. In the calculation, the refractive indexes of PMMA and PS were measured by a refractometer to be 1.49 and 1.60, respectively.

In Figures 4 and 5, the experimental and calculated curves are shown. Curve 4-B was calculated from eq. (4), assuming all $d_i$ values to be fixed at 0.325 $\mu$, the mathematical average of the radius distribution, whereas curve 4-C was weighted

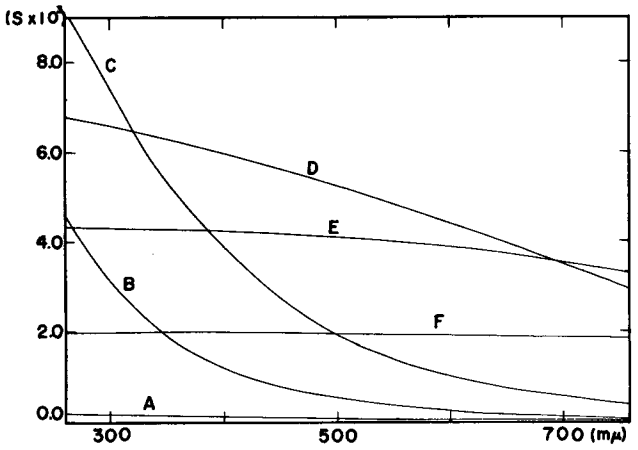


Fig. 6. Calculated scattering intensity $S$ for various $d$ values for PMMA and PS blend system: (A) $d = 0.025\ \mu$; (B) $d = 0.075\ \mu$; (C) $d = 0.125\ \mu$; (D) $d = 0.325\ \mu$; (E) $d = 0.525\ \mu$; (F) $d = 1.175\ \mu$.

by $f(d_i)$ of Figure 3. The porportionality constant in which the concentration term of the scattering elements was also included was so determined as for the calculated curves to coincide with the experimental value at 500 m$\mu$. It is clear that curve C calculated considering the effect of the radius distribution fits better the experimental curve 4-A.

The simulation curve shows a strong absorption in the short wavelength region and extends from UV to NIR, which is just the one observed in the colored opal sheet. The calculated absorption is slightly low in both the UV and NIR regions, but the result is satisfactory, considering various factors which will affect the light passing in the polymer system as well as the multiple scattering.

As for sample B, however, no secondary structures can be found (Fig. 1b or 1d) and the coloring is much less (Fig. 5). The calculated curve in regard to the St-MMA copolymer spheres (Fig. 5) also shows less coloring than sample A. The disagreement between the experimental and calculated value compared with the result of sample A must be caused by the fact that sample B is too thick for the multiple scattering to be neglected.

In Figure 6, the values $S$ calculated from eq. (4) for various $d$ values are plotted for the PMMA and PS blend system. When the scattering elements are small ($d = 0.0525\ \mu$), the scattering in the visible region is negligible. As the elements become larger from 0.075 to 0.125 $\mu$, both the scattering power and the difference of the scattering intensities between short and long wavelengths in this spectral range increase. When the elements become larger from 0.525 to 1.175 $\mu$, the dependence of the scattering intensity on the wavelength decreases, which results in less coloring.

From the discussions stated above, the coloring phenomena of opal sheet are well explained as structural color. The same treatment, of course, can be applied to the polymer system other than the PMMA and PS blend system.

The authors are much obliged to Dr. Kubota for his useful discussions and advice and to Mr. Shiraga of our laboratory for taking EM and SEM pictures.

## References

1. J. Tyndall, *Phil. Mag.*, **37**, 384 (1869).
2. G. Mie, *Ann. Phys.*, **25**, 377 (1908).
3. P. Debye, *Ann. Phys.*, **30**, 59 (1909).
4. G. Oster, *Chem. Rev.*, **43**, 319 (1948).
5. Van der Hulst, *Optics of Spherical Particles*, Drukkerij Duwaer and Zonen, Amsterdam 1946.
6. R. S. Stein and M. B. Rhodes, *J. Appl. Phys.*, **31**, 1873 (1960).
7. I. Inoue, M. Moritani, T. Hashimoto, and H. Kawai, *Macromol.*, **4**, 500 (1971).
8. R. Samuels, *J. Polym. Sci. C*, **13**, 37 (1966).
9. D. H. Clewell, *J. Opt. Soc. Amer.*, **31**, 521 (1941).
10. R. H. Sawter, *J. Appl. Phys.*, **13**, 596 (1942).
11. T. F. Anderson and A. G. Richards, Jr., *J. Appl. Phys.*, **13**, 748 (1942).
12. R. D. Heidereich and V. G. Peck, *J. Appl. Phys.*, **14**, 23 (1943).
13. C. Reinhold, F. W. Fischer, and A. Peterlin, *J. Appl. Phys.*, **35**, 71 (1964).
14. L. Rayleigh, *Proc. Roy. Soc.*, **A90**, 219 (1914).